

## Potential Energy Surface for H<sub>2</sub>O ... CO<sub>2</sub>

Patrícia Regina Pereira Barreto(PQ)<sup>1</sup>, Alessandra Ferreira. Albernaz (PQ)<sup>2</sup>, Eberth Correa<sup>3</sup>

prpbarreto@gmail.com, albernazalessandra@gmail.com, eberthcorrea@gmail.com

<sup>1</sup>Laboratório Associado de Plasma, Instituto Nacional de Pesquisas Espaciais, CP515, São José dos Campos, SP CEP 12247-970, Brazil, <sup>2</sup>Instituto de Física, Universidade Brasília, CP04455, Brasília, DF CEP 70919-970, Brazil, <sup>3</sup>Ciências Naturais Aplicadas, Universidade de Brasília, Campus do Gama, Gama, DF CEP 72444-240, Brazil

Keywords: Potential Energy Surface, H<sub>2</sub>O-CO<sub>2</sub>, second virial calculation

### INTRODUCTION

We have been working in the development of potential energy surface (PES) for several years. Basically, for system as AB-CD<sup>1</sup>, where A, B, C and D are atoms, that can equals or not, and H<sub>2</sub>O-X<sub>2</sub>, where X can be any atom<sup>2</sup>. Now, we propose a new surface, based in the H<sub>2</sub>O-X<sub>2</sub> PES for H<sub>2</sub>O ... CO<sub>2</sub>, according to:

$$V(R_{CM}, \alpha, \theta_1, \theta_2, \phi) = \sum_m F_m(\Omega) v_m(R_{CM})$$

Where  $R_{CM}$  is the distance between the centers of mass,  $F_m(\Omega)$  is an angular function and  $v_m(R)$  are the moments.

### METHODS

The system are treated as rigid motor, where the geometries of H<sub>2</sub>O and CO<sub>2</sub> are kept frozen in their equilibrium. Fig. 1 shows the coordinate system used.

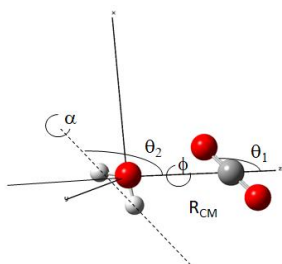


Fig 1: Coordinate system, where  $R_{CM}$  is the distance between the centers of mass (CM) of H<sub>2</sub>O and CO<sub>2</sub>,  $\theta_1$  is the angle of CO bond with the Z axis,  $\theta_2$  is the angle formed by the imaginary axis that pass through the CM of H<sub>2</sub>O and parallel to the line connecting the H atoms of H<sub>2</sub>O and the Z axis,  $\phi$  is the dihedral angle and  $\alpha$  is the angle that describes the rotation of H<sub>2</sub>O around the the line connecting the H atoms.

The angular function is written as:

$$F(\Omega) = \sum_i \omega_i(\alpha) \sum_{L_1, L_2, L} Y_{L_1 L_2}^{L, 0}(\theta_1, \theta_2, \phi)$$

Where  $\omega_i(\alpha)$  is a cosine expansion in  $\alpha$  angle,  $Y_{L_a L_b}^{L, 0}(\theta_1, \theta_2, \phi)$  represents the bipolar spherical harmonics. The angles  $(\alpha, \theta_1, \theta_2, \phi)$  are given in Fig. 1.

To determine the moments  $v_m(R_{CM})$ , we choose 18 leading configurations whose choice is due to physical and geometric considerations. These configurations are divided in three groups, each group for three different  $\alpha$  angle, as 0,  $\pi/2$  and  $\pi$ . In each group we have six configurations, as H( $\pi/2, \pi/2, 0$ ), L(0,0,0), T<sub>a</sub>( $\pi/2, 0, 0$ ), T<sub>b</sub>(0,  $\pi/2, 0$ ), Z( $\pi/4, \pi/4, 0$ ) and X( $\pi/2, \pi/2, \pi/2$ ).

### RESULTS

The H<sub>2</sub>O and CO<sub>2</sub> are optimized using the Gaussian code<sup>3</sup> for different basis set and the geometric and electrical properties were determined, the results as shown in Tab.1.

Table 1: Geometric and electrical properties of H<sub>2</sub>O and CO<sub>2</sub> calculated at aug-cc-pVDZ (aDZ), aug-cc-pVTZ (aTZ), aug-cc-pVQZ (aQZ), in comparison with experimental data.

	aDZ	aTZ	aQZ	Ref.
H <sub>2</sub> O				
$r_{OH}$	0.967	0.962	0.959	0.958
$A_{HOH}$	103.9	104.2	104.4	104.5
$E_{ZEP}$	13.34	13.40	13.47	12.88
$\mu$	1.995	1.970	1.963	1.857
$\alpha$	9.239	9.493	9.538	10.128
$\Theta$	12.553	12.509	12.488	13.184
IP	12.33	12.49	12.55	12.62
EA	0.69	0.56	0.51	1.20
PA	162.24	163.46	163.63	165.00
CO <sub>2</sub>				
$r_{CO}$	1.177	1.167	1.163	1.162
$A_{OCO}$	180	180	180	180
$E_{ZEP}$	7.11	7.21	7.26	7.17
$\mu$	0	0	0	0
$\alpha$	17.466	17.514	17.473	16.916
$\Theta$	41.288	39.722	39.129	27.452
IP	9.72	12.52	13.77	13.78
EA	3.70	3.81	4.23	-0.60
PA	122.79	151.35	0.00	129.20

As one can see the aQZ basis set are in good agreement with experimental data, and this base will set for future calculation.

Molpro and SAPT determined the Leading Configuration energies at aug-cc-pVQZ. Fig. 2(a) shows the results for few LC, while Fig. 2(b) compares the SAPT and Molpro energies for Ta LC with  $\alpha=\pi$ , and Fig. 2(c) shows the SAPT contribution.

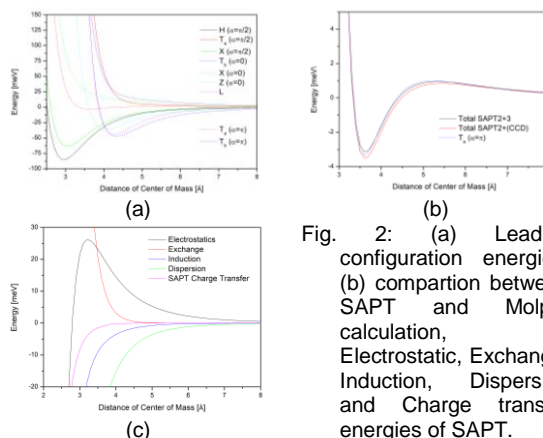


Fig. 2: (a) Leading configuration energies, (b) comparison between SAPT and Molpro calculation, (c) Electrostatic, Exchange, Induction, Dispersion and Charge transfer energies of SAPT.

### ACKNOWLEDGEMENTS

I thank FAPESP and FADF.